The Band Fluorescence of Mercury Vapor*

A. O. McCoubrey
University of Pittsburgh, Pittsburgh, Pennsylvania, and Westinghouse Research Laboratories, East Pittsburgh, Pennsylvania
(Received December 3, 1953)

The band fluorescence of mercury vapor excited by the 2537A atomic line has been studied during the afterglow. Time sampling techniques were employed to overcome difficulties attending the measurement of very low-intensity radiations. The two main band constituents (centered at 4850A and 3350A) were found to decay simultaneously under all conditions investigated. The temporal structure of the decaying fluorescence was found to be characterized by two time constants and has the form associated with chain types reactions. The two time constants and the relative intensities of the 4850A and 3350A bands were measured for a range of vapor densities at a fixed vapor temperature. In order to evaluate the role of diffusion in the lifetime of the excited particles involved, measurements were made in vessels of two different sizes.

The experimental results have led to an interpretation according to which the optically excited $Hg(^3P_1)$ atoms are converted into metastable $Hg(^3P_0)$ atoms by inelastic collisions. The $Hg(^3P_0)$ atoms are then converted in a three-body collision reaction to metastable $Hg_2(^3O_u^-)$ molecules which, in turn, may be destroyed in the vapor by either one of two processes, i.e., by spontaneous radiation to the ground state, giving rise to the 3350A band, or by a second three-body collision through which the emission of the 4850A band is induced. An analysis based upon this picture has permitted the quantitative evaluation of several properties of the particles involved. The diffusion coefficient of the $Hg(^3P_0)$ atom was found to be 210 cm²/sec for a density of 10^{16} atoms/cc and a temperature of 200°C; the diffusion coefficient of the $Hg_2(^3O_u^-)$ molecules is 88 cm²/sec under the same conditions. The spontaneous radiation rate of the $Hg_2(^3O_u^-)$ molecules is 20 sec^{-1} and the three-body collision induced radiation rate is 21×10^{-32} $(atoms/cc)^{-2}$ sec^{-1}. The three-body destruction rate for the $Hg(^3P_0)$ atoms is 100×10^{-32} $(atoms/cc)^{-2}$ sec^{-1}. It was also found that the $Hg_2(^3O_u^-)$ molecules are approximately 90 percent reflected by the glass walls of the enclosure. The diffusion coefficient obtained for $Hg(^3P_0)$ atoms is in agreement with the results of other work and the three-body collision rates are comparable with those for similar processes investigated elsewhere.

I. INTRODUCTION

WHEN mercury vapor is excited by the 2537A resonance line it emits, in addition to imprisoned resonance radiation,[1] a continuous band spectrum whose intensity depends strongly upon the vapor density. This band fluorescence[2] consists of two main constituents, one in the visible region centered at 4850A, and the second in the near ultraviolet region centered at about 3350A. The spectral distribution of these bands is shown in Fig. 1. A third band of much less intensity and smaller spectral extent is associated with the fluorescence at a wavelength of 2650A. When the radiation exciting the vapor is extinguished, there is an afterglow during which the fluorescent bands persist for several milliseconds. Phillips[3] first discovered the persistence and Rayleigh[4] carried out a number of qualitative studies using a moving vapor stream technique. In this work Rayleigh estimated the persistence times and found some evidence for the simultaneous decay of the 3350A and the 4850A components.

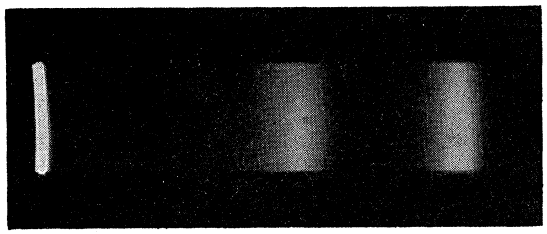

FIG. 1. The band fluorescence of mercury vapor at a density of about 6×10^{16} atoms/cc. The line on the left is the 2537A exciting line; the center band extends from about 3000A to 3700A with maximum intensity at 3350A; the band on the right extends from 4000A to 5300A with maximum intensity at 4850A.

Rayleigh later found that the 4047A mercury line was absorbed[5] by the fluorescing vapor and the visible triplet, 4047A, 4358A, and 5461A was thereby excited (see Fig. 2). He therefore concluded that metastable $Hg(^3P_0)$ atoms were present in the fluorescing vapor. From the absorption of the 5461A line he found that metastable $Hg(^3P_2)$ atoms were also present at much smaller concentration.

Frank and Grotrian[6] first associated the continuous bands with excited levels of the Hg_2 molecule. In a recent interpretation of the mercury vapor fluorescence, due to Mrozowski,[7] the 4850A band was considered to arise by direct radiation from the $Hg_2(^3O_u^-)$ state.[8] While this molecular state is metastable, a small but finite transition probability is considered to be due to the gyroscopic effect of molecular rotation which spoils the quantization of electronic angular momentum parallel to the internuclear axis. On account of the metastability, it was presumed that the $Hg_2(^3O_u^-)$ state acts as the primary reservoir for the long-lived molecular excitation. The 3350A band was accounted for in terms of transitions from the $Hg_2(^3\Sigma_u)$ state. This

* The research reported here was submitted to the Graduate School of the University of Pittsburgh in partial fulfillment of the requirements for the degree of Doctor of Philosophy. The work was performed at the Westinghouse Research Laboratories.

[1] T. Holstein, Phys. Rev. **72**, 1212 (1947).

[2] For a short survey and bibliography, see W. Finkelnburg, *Kontinuierliche Spektren* (Julius Springer, Berlin, 1938), Sec. 60.

[3] F. S. Phillips, Proc. Roy. Soc. (London) **A89**, 39 (1913).

[4] Lord Rayleigh, Proc. Roy. Soc. (London) **A114**, 620 (1927).

[5] Lord Rayleigh, Proc. Roy. Soc. (London) **A137**, 101 (1932).

[6] J. Frank and W. Grotrian, Z. Physik **4**, 89 (1921).

[7] S. Mrozowski, Z. Physik **106**, 458 (1937).

[8] The classification of the electronic states of diatomic molecules adopted here is described in G. Herzberg, *Spectra of Diatomic Molecules* (D. Van Nostrand Company, Inc., New York, 1950).

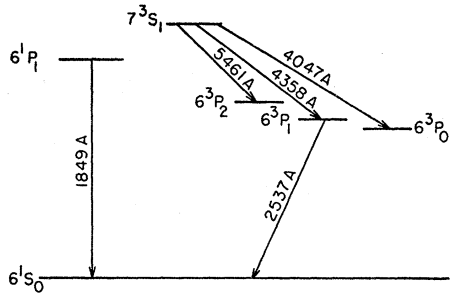

FIG. 2. The energy levels of mercury.

state is thought to have a lifetime of the order of 10^{-7} second. The persistence of the 3350A band was held to be due to a continual repopulation of the $Hg_2(^3\Pi_u)$ state from the lower-lying $Hg_2(^3\Sigma_u^-)$ reservoir as a result of inelastic collisions. Because of the short lifetime of the $Hg_2(^3\Pi_u)$ state, both bands were considered to decay with the population of $Hg_2(^3\Sigma_u^-)$. In this way the common persistence times of the 3350A band and the 4850A band were explained as required by the experiments of Rayleigh.

Recently, in this laboratory, the fluorescence of mercury vapor was observed in connection with experiments on the imprisonment of resonance radiation.[9] While the apparatus was not well suited to the study of fluorescence, several significant observations were made. It was confirmed that the 3350A band and the 4850A band decay together. At constant vapor temperature, the persistence time was found to decrease rapidly as vapor density increased. However, at constant vapor density the temperature had no observable effect on the persistence. It was also found that the intensity of the 4850A band relative to that of the 3350A band, $I(4850)/I(3350)$, increased with vapor density. This result is in agreement with a similar observation by Mrozowska.[10]

The experimental observations have shown the Mrozowski picture to be incorrect in several respects. In particular, it is of interest to note that the rate of transitions from the $Hg_2(^3\Sigma_u^-)$ reservoir to the $Hg_2(^3\Pi_u)$ state would be expected to increase with temperature with a consequent decrease in persistence time. As mentioned previously, such a decrease is not observed. Also, an increase in vapor density would be expected to increase the frequency of transitions from the $Hg_2(^3\Sigma_u^-)$ state to the $Hg_2(^3\Pi_u)$ state. As a result, $I(4850)/I(3550)$ should decrease with an increase in vapor density. The experiments reveal that the opposite occurs.

In order to lay the groundwork for a better theoretical explanation, an experimental program was undertaken to obtain quantitative information concerning the persistent band fluorescence of mercury vapor. The present paper describes these experiments and presents the results within the framework of new theoretical hypotheses.

[9] Holstein, Alpert, and McCoubrey, Phys. Rev. **76**, 1259 (1949).
[10] I. Mrozowska, Acta. Phys. Polonica **2**, 81 (1933).

II. EXPERIMENTAL METHOD

a. General Technique

In the experimental method, a vessel containing mercury vapor is irradiated with 2537A resonance radiation. After a time interval during which the concentration of imprisoned resonance radiation builds up in the vessel, the incident light is turned off. The afterglow contains not only the escaping resonance radiation, but also the continuous bands associated with the persistent fluorescence. Through the use of optical filters these different spectral components may be separated for individual study.

The detailed procedure may be understood with reference to the block diagram in Fig. 3. Radiation from a mercury discharge lamp is periodically interrupted by a rotating shutter. A monochromator selects the 2537A resonance line and focuses it on a cylindrical tube containing mercury. This vessel, the "fluorescence tube," is surrounded by a furnace which controls the temperature and pressure of the mercury vapor. The intensity of radiation emitted by the vapor in the fluorescence tube is measured by means of an electron-multiplier phototube. Optical filters are used in front of the phototube to separate the band fluorescence from imprisoned resonance radiation, and also to resolve the band spectrum. The intensity signal from the photomultiplier tube is indicated by a method to be discussed in detail in later paragraphs. The indicating circuits are synchronized to operate during the afterglow periods by a trigger voltage derived photoelectrically from the rotating shutter.

The fluorescence tubes were of cylindrical geometry having a length at least ten times the radius. The main body of the tube was made of Corning 7911 glass which is transparent to the ultraviolet radiation used for excitation. The lower end of the tube, which served as the reservoir for liquid mercury, included a graded seal terminating in Pyrex glass. This construction permitted the tubes to be prepared on a standard Pyrex vacuum system. Using techniques described in detail by Alpert,[11] the tubes were evacuated and filled with triply

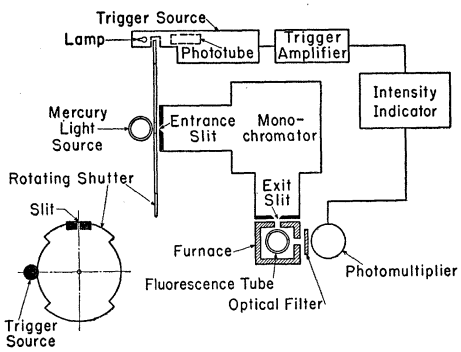

FIG. 3. The schematic diagram of the apparatus.

[11] D. Alpert, J. Appl. Phys. **24**, 860 (1953).

distilled mercury. At the time of sealoff the pressure of residual gases was never greater than 10^{-8} mm Hg.

Fluorescence tubes having two different sizes were prepared. The larger tube was 2.35 cm in radius and 25 cm long, and the smaller tube was 0.64 cm in radius and 14 cm long.

To accomodate the two fluorescence tube sizes, two furnaces of similar design were constructed. Figure 4 is a sketch showing the important details of the larger furnace. The furnace consisted of an upper and lower section, both of which were constructed of heavy copper cylinders. The heating element consisted of nichrome wires embedded in the walls of the cylinders with quartz tubing for electrical insulation. The heating elements in the two sections were supplied from independent current sources. Thus the pressure of mercury vapor in equilibrium with the liqiud was controlled by the temperature of the lower section, while the vapor temperature above was that of the upper furnace section. To prevent drafts of cool air from entering the furnace, quartz windows covered the openings in the upper section through which passed the incident exciting light and the emerging radiation. Temperatures were measured with thermocouples strapped to the glass as illustrated.

The optical filters used to resolve the fluorescent radiation were Corning 5840 for the 3350A band and Corning 3389 for the 4850A band. Data supplied by the manufacturer indicated that each filter allowed less than one percent of the rejected band to pass, while transmission of the 3350A band was about 50 percent and transmission of the 4850A band was about 85 percent.

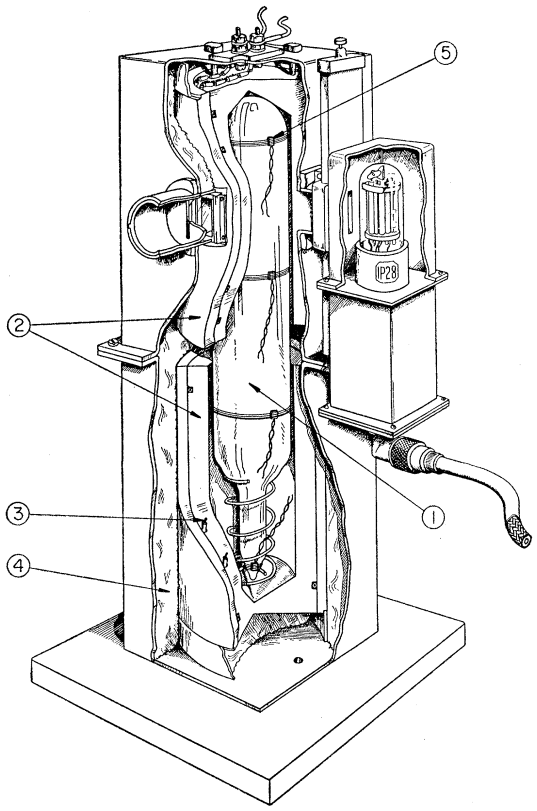

FIG. 4. The furnace and fluorescence tube details: 1. fluorescence tube; 2. copper heating units; 3. heating element; 4. thermal insulation; 5. thermocouple.

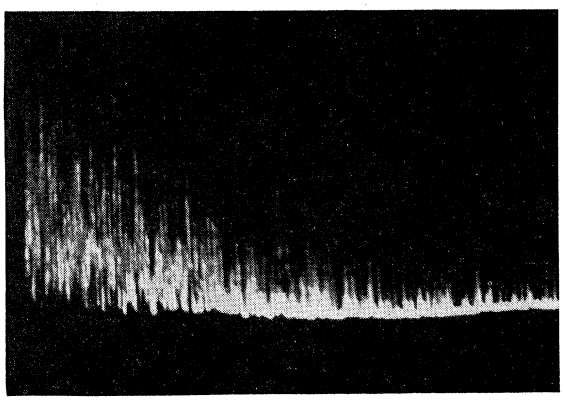

FIG. 5. An oscilloscope trace of a fluorescence decay cycle. The shot effect is due to the random arrival of optical quanta at the photomultiplier. The trace in this photo is about 30 milliseconds long.

b. Time Sampling Technique

In the preliminary experiments,[6] the intensity signals from the photomultiplier were indicated directly on an oscilloscope. Thus one observed a continuously decaying signal; a photograph of a typical trace is given in Fig. 5. While even these traces represented new data, they were obviously not suitable for good quantitative measurements. The very low optical intensities involved and the consequent statistical variations or "shot effect" made such a method inadequate for the observation of the fine structure in the decay. The limitations imposed by the statistics in the decaying radiation presented the outstanding experimental problem in the research. To meet this problem, a time sampling technique was devised in which the circumstance that a photomultiplier tube is sensitive only when proper voltages are applied to its electrodes is used to advantage.

The operation of the time sampling technique may be discussed with reference to Figs. 6A and 6B, in which the voltage applied to the photomultiplier is shown in its phase relationship to a hypothetical time varying light signal. In Fig. 6A, the photomultiplier supply voltage is gated on for a short fixed time interval, Δt, at a relative time $t=t_1$. The charge which flows from the photomultiplier tube under these conditions during one cycle is

$$q(t_1)=AG\int_{t_1-\frac{1}{2}\Delta t}^{t_1+\frac{1}{2}\Delta t} I(t)dt,$$

where A is the calibration factor which relates the instantaneous photocathode current to the instantan-

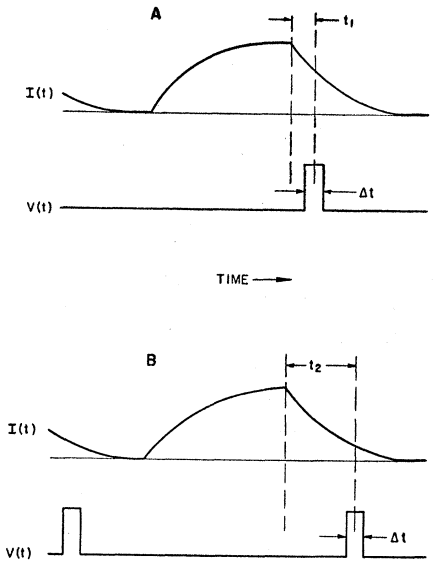

FIG. 6. Time sampling of light signal.

eous light intensity and G is the photomultiplier gain. The charge $q(t_1)$ is proportional to the average intensity during the time interval $(t_1-\frac{1}{2}\Delta t)<t<(t_1+\frac{1}{2}\Delta t)$, and for Δt sufficiently small this charge may be used as a measure of $I(t_1)$. As indicated in Fig. 6B, the intensity $I(t_2)$ at a relative time $t=t_2$, is obtained by relative displacement of the photomultiplier voltage gate. Thus, the time dependence of the radiation intensity may be obtained by a point by point procedure.

If the intensity $I(t)$ contains large random fluctuations, which is the case of interest here, it is necessary to collect a sufficient number of photomultiplier charge samples $q(t_1)$ to obtain an average over the fluctuations. This procedure amounts to taking intensity samples at a selected relative time t from a large number of intensity cycles which are identical in every respect except for the random fluctuations; the average sample value then yields the required experimental point. By this method, the average time dependence of an intensity variation may be obtained which contains fluctuations having a mean period large compared to the period of the intensity variation. If the mean intensity for a given relative time t is $\langle I(t)\rangle_{Av}$, the root-mean-square deviation expected in a series of charge measurements each of which requires S intensity cycles to obtain is $\delta=[A\langle I(t)\rangle_{Av}\Delta tS/e]^{\frac{1}{2}}$, and the fractional error in the information is

$$e\delta/A\langle I(t)\rangle_{Av}\Delta tS=[A\langle I(t)\rangle_{Av}\Delta tS/e]^{-\frac{1}{2}},$$

where e is the electronic charge.

An example may serve to better establish the ideas above. Consider a case in which it is desired to measure the time dependence of a decay which extends over a time interval of ten milliseconds. To resolve the fine structure of such a decay, it might be necessary to use a photomultiplier gate interval $\Delta t=0.1$ millisecond. The limit of useful sensitivity of a photomultiplier tube depends upon its dark current which, for a selected RCA Type 1P28 photomultiplier operating at a gain of 10^6, may be 10^{-9} ampere. In the case of an easily measured instantaneous signal current of ten times this dark current, the instantaneous primary photoelectric current is about 5×10^4 electrons/second, or about five photoelectrons during one gate interval Δt. If these five electrons are regarded as a measure of the instantaneous intensity, the root mean square error will be about 45 percent. However, if the photoelectrons which are emitted during 1000 identical gate intervals are collected the rms error may be reduced almost to one percent. Since the quantum efficiency of the photosurface in the Type 1P28 phototube is about ten percent in the ultraviolet,[12] the optical radiation intensity considered in this example corresponds to about 50 quanta entering the photomultiplier during each gate interval Δt.

It should be pointed out that the preceding considerations neglect the statistics in the electron multiplication process in the phototube. This effect is due to the random fluctuations in the number of secondary electrons emitted from the phototube dynodes per incident primary electron. An estimate based upon an analysis by Shockley and Pierce[13] indicates that this source of noise is small compared to the "shot effect" considered above.

The additional components required for the sampling technique are shown in Fig. 7. Gate voltage for the photomultiplier was obtained from an electronic generator whose action was initiated by the trigger voltage from the rotating shutter. This trigger voltage established the reference time in the optical decay cycles. To allow for the rough adjustment of the relative time

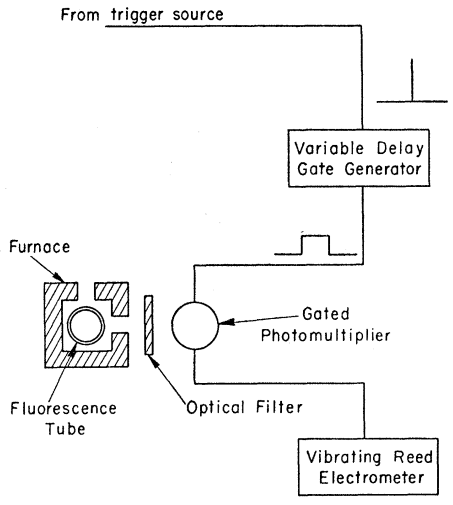

FIG. 7. Schematic diagram of apparatus for the time sampling of optical radiation intensities.

[12] V. K. Zworykin and E. G. Ramberg, *Photoelectricity and Its Application* (John Wiley and Sons, Inc., New York, 1949).
[13] W. Shockley and J. R. Pierce, Proc. Inst. Radio Engrs. **26**, 321 (1938).

of the trigger, the angular position of the trigger source was adjustable about the axis of the rotating shutter. In addition, the gate generator was equipped with a manual control by means of which the gate could be electrically delayed relative to the trigger for any period up to half of an optical cycle. The width of the gate voltage was adjustable from 0.05 to one millisecond. Charge samples from the photomultiplier tube were collected on a capacitor whose potential was measured by a vibrating reed electrometer.

The relative occurrence time of the photomultiplier gate was measured by observing its position relative to the beginning of the optical decay cycle with the aid of a cathode-ray synchroscope. The time axis of the synchroscope was continuously calibrated by means of an accurate time mark generator.

It may here be remarked that gating a photomultiplier is not only a convenient way to achieve time sampling, but it also provides a method for observing very weak optical signals immediately following intense phenomena. This technique is free of the saturation effects which render sensitive wideband electronic amplifiers inoperative for relatively long periods of time following intense signals. While these difficulties have been overcome by gating the amplifier or by other special techniques, it is usually more convenient to gate the photomultiplier. The time resolution available depends upon the speed of application and removal of the gate voltage. With modern pulse-generating techniques the method may be extended to study very fast optical phenomena.

One of the major sources of uncertainty in the experiment was in the determination of the vapor density. Vapor densities were obtained from the temperature of the mercury reservoir on the fluorescence tube by the use of saturated vapor pressure data given in Landolt-Börnstein.[14] These density values were adjusted to take into account the higher temperature in the observation region. To maintain vapor densities constant within ten percent during a decay measurement, it was necessary to keep the temperature constant within 2°C. To accomplish this the heating elements were supplied from a current source which was regulated to one percent, and the furnace was allowed to reach steady state by waiting at least two hours before making a measurement. Precautions were also taken to keep the exterior environment of the furnace at constant temperature. These measures served to limit the uncertainties in vapor density to $2\frac{1}{2}$ percent at a density of 4×10^{16} atoms/cc and to a maximum of ten percent at 10^{16} atoms/cc.

Another source of error which must be considered concerns the intensity measurements. Uncertainties due to shot fluctuations could, in principle, be reduced to any desired extent by taking a sufficient number of intensity samples. However, limitations were encountered due to fluctuations in photomultiplier gain as a result of variations in gate pulse voltage and fluctuations in intensity of the 2537A source of excitation. It is felt that, due to all causes, uncertainties in intensity measurements amounted to no more than three percent.

[14] Landolt-Börnstein, *5 Auflage II* (Julius Springer, Berlin, 1923), p. 1334.

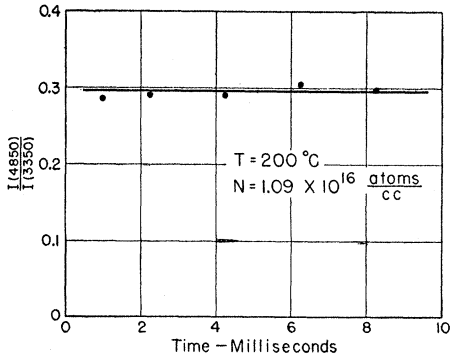

FIG. 8. The relative intensity of the visible and near ultraviolet bands in the afterglow. The curve demonstrates the simultaneous decay of the two bands.

III. RESULTS

The early experimental work indicated several aspects of the band fluorescence which required quantitative investigation. In the first place, it was of interest to check carefully the result that the radiation in the two principal bands decays simultaneously. Also, since early experiments had shown strong pressure effects, it seemed imperative to obtain quantitative data on the density variation of the band intensities as well as the persistence times. Finally, the long persistence times encountered in the mercury fluorescence suggested that diffusion might be an important feature. In order to make a thorough test of this possibility, the experiments were carried out in fluorescence tubes of two different sizes. Measurements were made with a vapor temperature of 200°C; as a result of this choice the vapor temperature remained in excess of the mercury condensation temperature over a wide range of densities.

The ratio of the intensity of the 4850A band to that of the 3350A band was measured at various times in the afterglow and for different vapor densities. For all mercury vapor densities investigated, i.e., for densities between 7×10^{15} atoms/cc and 5×10^{16} atoms/cc, this ratio was found to be constant with respect to time in the afterglow period. This particular result was also obtained for several vapor temperatures between 150°C and 200°C. A plot of measurements made for a density of 1.09×10^{16} atoms/cm^3 and a temperature of 200°C is given in Fig. 8.

The variation with vapor density of the ratio, $I(4850)/I(3350)$, as measured during the afterglow is given in Fig. 9.

The intensity of fluorescent radiation as a function of time in the afterglow was measured using the large

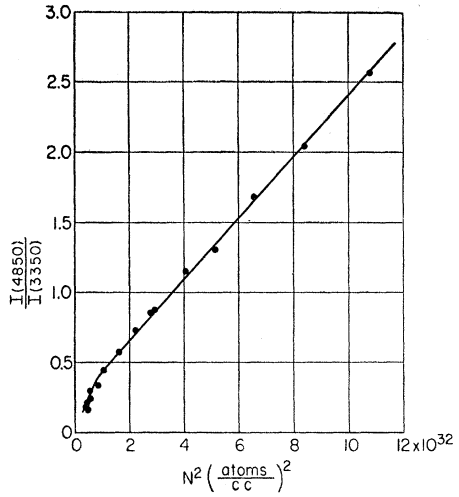

FIG. 9. The ratio of the band intensities as a function of the square of the vapor density.

(2.35-cm radius) tube. Since the intensity of the two bands had previously been found to decay simultaneously, the total radiation from the 3350A and the 4850A bands was included in these measurements. A Corning 7740 filter (Pyrex glass) was used to cut out the imprisoned resonance radiation escaping during the initial stages of the decay.

Figure 10 illustrates the data of a typical decay measurement taken with a photomultiplier sampling gate width of 100 μsec. As indicated, the curve consists of an initial relatively slow decay rate, going finally into a constant slope characteristic of the exponential form. It is found that the difference $\Delta I(t)$ between the final decay curve extrapolated to early time and the actual decay curve is also exponential in nature. These decay

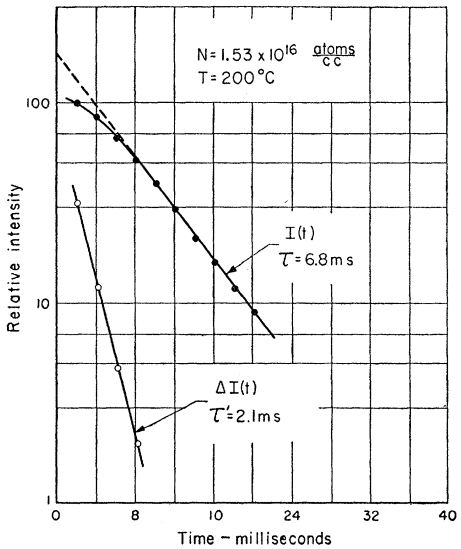

FIG. 10. The measured intensity $I(t)$ and difference intensity $\Delta I(t)$ in the afterglow of Hg_2 fluorescence.

curves, are therefore, characterized by an initial time constant τ_1' and a fina time constant τ_1 both of which depend upon the vapor density. Tables I and II give the values τ_1' and τ_1 measured at different densities for the constant vapor temperature of 200°C.

The effect of enclosure geometry on the rate of fluorescence decay was evaluated by comparing the rate of decay of radiation from the large tube with that emitted by the smaller tube (0.64-cm radius). Table III lists the values of the final time constant τ_2 for decays in the small tube. To facilitate a comparison of the observations, the same values of vapor temperature and density were used in both tubes. Typical data comparing the decays are plotted in Fig. 11. In the case of the small tube, the initial structure of the decay was too fast to measure accurately with the equipment designed for the longer decays.

IV. DISCUSSION

The more complete experimental information just described has made new theoretical considerations possible. Before discussing these in detail it is desirable to review some consequences of the experiments.

TABLE I. Density dependence of the final time constant τ_1 associated with the decay of fluorescence in the large tube. $T = 200$°C.

M (atoms/cc)	τ_1 (sec)
1.17×10^{16}	7.2×10^{-3}
1.53	6.8
1.91	6.25
2.00	5.8
2.56	4.2
2.56	4.3
3.18	3.1
3.58	2.35
4.19	1.82

If the 4850A band and the 3350A band had their origins in different excited molecular reservoirs, the persistence of each band would depend upon the depopulation rate of its associated reservoir. The circumstance that the two bands decay simultaneously, therefore, suggests the hypothesis that there is a common persistent reservoir of molecular excitation which feeds both bands. Furthermore, the complex decays which are observed in the afterglow are characteristic of chain reactions involving "parent-daughter" processes. The fact that two exponential parameters are associated with the decay suggests two reservoirs of excitation, one feeding the other which, in turn, radiates the observed fluorescent bands.

Figure 11 demonstrates the strong influence which enclosure size has on the persistence time of the fluorescence. This result suggests that diffusion plays a part in determining the lifetimes of the persistent reservoirs.

The influence which the vapor density exerts upon the persistence time is evident in Tables I and II. This data was taken in the larger tube in which diffusion

would be expected to play a relatively less important role. The increase in the rate of decay with the vapor density indicates that collision destruction processes affect the life of both persistent reservoirs. The operation of a collision process is also evident in Fig. 9, which gives the density dependence of the relative intensities of the 4850A band and the 3350A band.

Finally, it should be noted that the entire fluorescence phenomenon is density dependent. Though further quantitative measurements have not been made, it has been observed that while band radiation is detected with difficulty at a density of 6×10^{15} atoms/cc, it becomes easily detectable at a density of 1×10^{16} atoms/cc and the total intensity continues to increase.

The generalities discussed above have led to an interpretation suggested by Holstein. According to this interpretation, the first stage leading to the fluorescence is the absorption of the mercury resonance radiation by normal $Hg(^1S_0)$ atoms

$$h\nu(2537)+Hg(^1S_0)\rightarrow Hg(^3P_1). \quad (1)$$

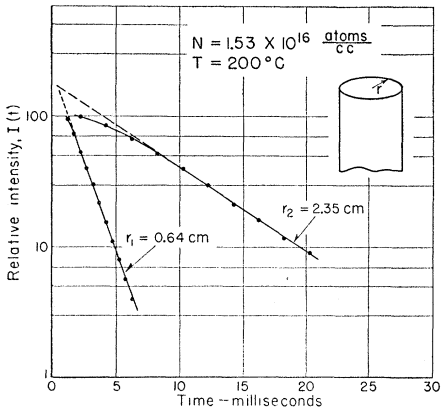

FIG. 11. The effect of geometry on the rate of fluorescence decay.

As a consequence of the imprisonment of resonance radiation,[15] the effective lifetime of a quantum of 2537A radiation is of the order of 100 microseconds in the enclosures considered. Knowing the excitation power entering the fluorescence tube, one can compute that the concentration of $Hg(^3P_1)$ builds up to the order of 10^{10} (atoms/cc).

The next step in the process is considered to be the collision conversion of resonance atoms to metastable atoms, which constitute the nonradiating reservoir of excitation, i.e.,

$$Hg(^3P_1)+Hg(^1S_0)\rightarrow Hg(^3P_0)+Hg(^1S_0)+0.21 \text{ ev}. \quad (2)$$

The presence of $Hg(^3P_0)$ metastable atoms in the fluorescing vapor has been observed,[5] and it has long been known[16] that such metastables may be created as a result of the collision quenching of the $Hg(^3P_1)$ resonance state.

[15] T. Holstein, Phys. Rev. **72**, 1212 (1947).
[16] W. Arthman and P. Pringsheim, Z. Physik **35**, 626 (1926).

TABLE II. Density dependence of the initial time constant τ_1' associated with the decay of fluorescence in the large tube. $T=200°C$.

N (atoms/cc)	τ_1' (sec)
1.53×10^{16}	2.1×10^{-3}
1.91	2.0
2.00	2.37
2.56	1.4
3.58	0.75

As the third step, it is postulated that metastable atoms are converted to metastable diatomic molecules by three-body collisions

$$Hg(^3P_0)+2Hg(^1S_0)\rightarrow Hg_2(^3O_u^-)+Hg(^1S_0). \quad (3)$$

These diatomic molecules are considered to be the radiating reservoir mentioned above. The mechanics of this reaction may be outlined with reference to the potential energy diagram in Fig. 15. The considerations upon which this diagram is based will be taken up later; it is sufficient now to point out that the first excited level, $Hg_2(^3O_u^-)$ arises from the $Hg(^1S_0)$ and the $Hg(^3P_0)$ states of the separated atoms. In reaction (3) it is considered that an atom $Hg(^1S_0)$ collides with a metastable $Hg(^3P_0)$ atom. While these atoms are in close association a third body $Hg(^1S_0)$ also collides, taking away enough energy to stabilize the system in a vibrational state of the electronic $Hg_2(^3O_u^-)$ configuration.

It is next proposed that the 3350A band arises from spontaneous radiation by the metastable molecules

$$Hg_2(^3O_u^-)\rightarrow 2Hg(^1S_0)+h\nu(3350). \quad (4)$$

While the $Hg_2(^3O_u^-)$ state is metastable according to molecular theory,[17] it is considered possible that the metastability may be slightly broken down as the result of a gyroscopic disturbance of the electronic motion arising from the nuclear rotation.[6,18,19]

The 4850A band is explained as arising from an alternate mode of decay of the $Hg_2(^3O_u^-)$ state, namely,

TABLE III. Density dependence of the final time constant τ_2 associated with the decay of fluorescence in the small tube. $T=200°C$.

N (atoms/cc)	τ_2 (sec)
1.17×10^{16}	1.45×10^{-3}
1.53	1.57
1.91	1.65
2.00	1.6
2.56	1.70
2.56	1.65
3.18	1.6
3.58	1.45
4.06	1.35

[17] G. Herzberg, *Spectra of Diatomic Molecules* (D. Van Nostrand Company, Inc., New York, 1950).
[18] S. Mrozowski, Revs. Modern Phys. **16**, 160 (1944).
[19] This effect will be referred to more briefly hereafter as "gyroscopic perturbation."

collision induced radiation

$$Hg_2(^3O_u^-)+2Hg(^1S_0)\rightarrow 4Hg(^1S_0)+h\nu(4850). \quad (5)$$

The participation of two normal mercury atoms in this reaction is required to explain the N^2 dependence of the intensity ratio, $I(4850)/I(3350)$, as well as the effect of the higher densities on the persistence time. While there may be intermediate steps in reaction (5), there is so far no experimental evidence by which they might be identified. Since the 4850A band and the 3350A band decay at the same rate, whatever intermediate steps may be involved must consume a very small amount of time compared to the lifetime of $Hg_2(^3O_u^-)$.

Proceeding to a quantitative description of the theory, it is possible to set up the differential equations which describe the population of the excited particles in the volume elements of the enclosure. While the imprisonment time of the resonance radiation is about 100 microseconds, this is small compared to the milliseconds required for fluorescence decay. Hence, the simplifying assumption may be made that at time zero, that is, when the exciting radiation is cut off, the concentration of $Hg(^3P_1)$ drops immediately to zero and the production of $Hg(^3P_0)$ ceases. It is then necessary to specify first, the rate at which metastable $Hg(^3P_0)$ atoms are lost, and second, the rate at which metastable $Hg_2(^3O_u^-)$ molecules are lost.

In a given volume element of the enclosure, metastable atoms are lost by diffusion to neighboring volume elements and by collision destruction according to reaction (3). In equation form these losses are given by

$$\partial m/\partial t = D_m\nabla^2 m - C_m N^2 m, \quad (6)$$

where m is the density of $Hg(^3P_0)$ atoms, D_m is the diffusion coefficient of these metastable atoms, and C_m is a constant of proportionality. The first term on the right represents the rate of change of density due to diffusion, while the second term expresses the rate of collision destruction of metastable $Hg(^3P_0)$ atoms. Because two normal atoms are involved in a collision with one metastable atom, the second term depends upon the square of the vapor density N and is linearly proportional to m.

Equation (6) can readily be solved for a given initial distribution of metastable $Hg(^3P_0)$ atoms in a cylindrical enclosure of length L and radius R, under the condition shown to be reasonable by Coulliette[20] that the metastable atoms are destroyed upon reaching the boundary. The solution is given by

$$m(r,t) = m_0(r)e^{-t/\tau'}, \quad (7)$$

where

$$1/\tau' = D_m[(2.41/R)^2+(\pi/L)^2]+C_m N^2, \quad (8)$$

and the quantity $m_0(r)$ specifies the initial spatial distribution of $Hg(^3P_0)$ atoms. In Eq. (7) and Eq. (8), it is assumed that the fundamental mode of the decay is predominant. The justification of this assumption rests upon the fact that the experimentally measured fluorescence decays could be resolved into two clearly exponential components (see Fig. 10). If higher modes were important, the logarithmic plots for the late parts of $I(t)$ and $\Delta I(t)$ would be expected to be nonlinear.

The metastable $Hg_2(^3O_u^-)$ molecules in any given volume element are lost by diffusion, by spontaneous radiative decay, and by collision induced radiation. In addition, $Hg_2(^3O_u^-)$ molecules are created according to reaction (3). These processes are expressed by the equation

$$\partial M/\partial t = D_M\nabla^2 M - BM - C_M N^2 M + C_m N^2 m, \quad (9)$$

where M is the density of $Hg_2(^3O_u^-)$ molecules, D_M is their diffusion coefficient, and B and C_M are factors of proportionality. The first term on the right represents the rate of change of molecular density due to diffusion. The second term represents the loss due to spontaneous radiation according to reaction (4). Since only one molecule is involved, this loss is proportional to the population, M, of $Hg_2(^3O_u^-)$ molecules. The third term represents the loss due to collision destruction according to reaction (5). Because two normal atoms interact with one molecule in this process, the third term depends upon the square of the vapor density and the first power of the $Hg_2(^3O_u^-)$ density. Finally, the term $C_m N^2 m$, which was a destruction term in Eq. (6), is a supply term in Eq. (9).

Equation (9) can also be solved for a cylindrical enclosure of radius R and length L. However, the condition with regard to destruction of $Hg_2(^3O_u^-)$ molecules at the walls is somewhat different than the complete destruction condition which is known to be accurate in the case of the metastable $Hg(^3P_0)$ atoms. This situation first became evident when Eq. (9) was solved assuming complete destruction at the walls. When the solution was compared with the experimental data, it was found that the density dependence of the diffusion loss was correctly predicted at high densities, but not at the lower densities. Experiment and theory were brought into good agreement by assuming that a fraction A of the moecules which strike the bounding walls are destroyed, while the remainder $(1-A)$ are reflected back into the interior of the enclosure.

Quantitatively, the incomplete destruction boundary condition may be expressed in terms of the molecular diffusion current reaching the walls. The current density of excited molecules striking the walls is given to a sufficiently good approximation by the kinetic theory relation $M\bar{v}/4$, where $\bar{v}$ is the mean molecular speed. The net current density to the walls is, then, $\frac{1}{4}M\bar{v}A$. The desired boundary condition is obtained by equating this quantity to the diffusion current density; thus, at the walls,

$$-D_M\nabla M = \tfrac{1}{4}M\bar{v}A. \quad (10)$$

[20] J. H. Coulliette, Phys. Rev. **32**, 636 (1928).

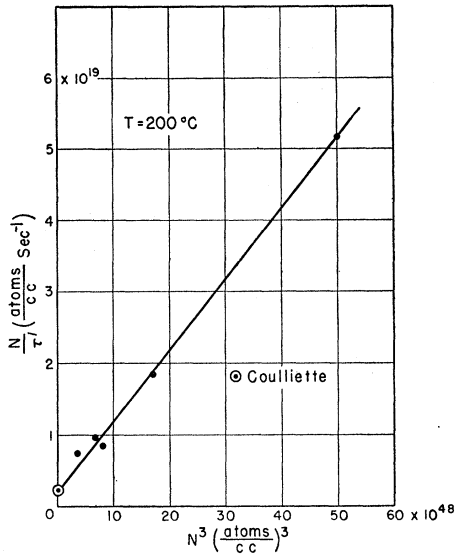

FIG. 12. The destruction of metastable mercury atoms, $Hg(^3P_0)$, in mercury vapor.

With the above boundary conditions, the solution of Eq. (9) is

$$I(t) \propto M(t) = \frac{\text{constant}}{\tau - \tau'}[\tau e^{-t/\tau} - \tau' e^{-t/\tau'}], \quad (11)$$

where

$$1/\tau = D_M[(j/R)^2 + (\pi/L)^2] + B + C_M N^2. \quad (12)$$

The quantity j is the first root of the equation,[21]

$$jJ_1(j) - \frac{R\bar{v}A}{4D_M} J_0(j) = 0, \quad (13)$$

where J_1 and J_0 are the Bessel functions of order one and zero, repectively. A mode analysis has been used and again, in Eqs. (11)–(13) it has been assumed that the fundamental decay mode predominates.

It should be noted that while Eq. (11) has the same form as the experimental decays, there is nothing in the theory to indicate whether τ or τ' is the larger time constant. It has already been implied that τ, which has been identified with the $Hg_2(^3O_u^-)$ molecules, is the larger of the two. However, the justification of this identification rests upon the experimental results. In particular, it will be shown that this choice results in the correct prediction of the diffusion coefficient for the metastable $Hg(^3P_0)$ atoms.

In order to compare the experimental time constants associated with $\Delta I(t)$ in Table II with the theory, it is convenient to rewrite Eq. (11) as follows

$$K\tau e^{-t/\tau} - I(t) = K\tau' e^{-t/\tau'}, \quad (14)$$

where K is a constant. The quantity on the left now corresponds to the experimental $\Delta I(t)$. To further facilitate the comparison, Eq. (8) is multiplied by N:

$$N/\tau' = ND_m[(2.41/R)^2 + (\pi/L)^2] + C_m N^3. \quad (15)$$

In this form N/τ' depends linearly on N^3 because ND_m is constant. The zero density intercept is related to the diffusion coefficient. In Fig. 12, the experimental data has been plotted in this way. The zero density intercept yields a value, $ND_m = 2.1 \times 10^{18}$ (atoms/cc) (cm²/sec) for a temperature of 200°C. It is of interest to compare this value with other experimental results. Measurements have been made for $Hg(^3P_0)$ atoms by Coulliette[20] whose result, corrected to the above temperature assuming a constant mean free path, is $ND_m = 2.11 \times 10^{18}$ (atoms/cc) (cm²/sec). Biondi[22] has obtained a value of $ND_m = 1.7 \times 10^{18}$ (atoms/cc) (cm²/sec) for the nearby $Hg(^3P_2)$ metastable state. This value is also corrected to a temperature of 200°C. This good agreement constitutes strong evidence for the correctness of the basic concepts of the theory.

For $t > \tau'$ the first term on the right side of Eq. (11) predominates and $\log I(t)$ becomes a straight line on a time plot. The slope of the line is $1/\tau$. This characteristic behavior is demonstrated by the data as shown in Fig. 10. The variation of τ with density is given for the large tube in Table I, and for the small tube in Table III.

Equation (12) may be applied to the large (subscript 1) and small (subscript 2) fluorescence tubes, yielding

$$1/\tau_1 = D_M[(j_1/R_1)^2 + (\pi/L_1)^2] + B + C_M N^2, \quad (16)$$

$$1/\tau_2 = D_M[(j_2/R_2)^2 + (\pi/L_2)^2] + B + C_M N^2. \quad (17)$$

Subtracting (16) from (17) and multiplying the result

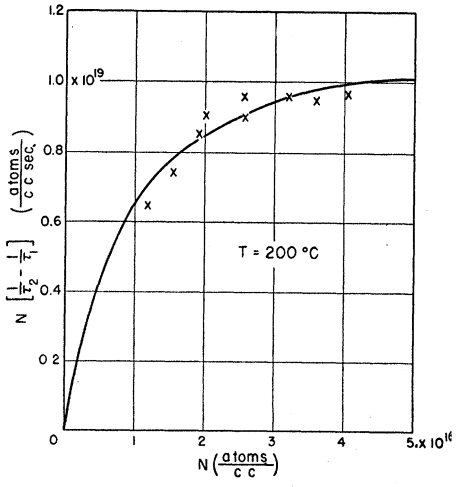

FIG. 13. The destruction of the diatomic mercury molecules at the enclosure walls. The solid curve is obtained from diffusion theory which includes a destruction coefficient at the walls of $A = 0.11$ and a density-diffusion coefficient product of $ND_M = 0.88 \times 10^{18}$(atoms/cc)(cm²/sec) at 200°C.

[21] Solutions of Eq. (13) are tabulated in H. S. Carslaw and J. C. Jaeger, *Conduction of Heat in Solids* (Oxford University Press, London, 1947), p. 379.

[22] M. A. Biondi, Phys. Rev. **90**, 730 (1953).

by N leads to

$$N\left(\frac{1}{\tau_2}-\frac{1}{\tau_1}\right)$$

$$=ND_M\left[\left(\frac{j_2}{R_2}\right)^2-\left(\frac{j_1}{R_1}\right)^2+\left(\frac{\pi}{L_2}\right)^2-\left(\frac{\pi}{L_1}\right)^2\right]. \quad (18)$$

The extra factor of N is included for convenience since ND_M is constant. The right-hand side of Eq. (18) depends upon N only through j_1 and j_2. It is also these quantities that bring in the effect of reflection of the molecules from the bounding walls. It is worth noting that if the molecules were entirely destroyed upon striking the walls, j_1 and j_2 would both become the first root of the Bessel function of order zero. In this case the right-hand side of Eq. (18) would be constant.

Using the data in Tables I and III, the values of $N(1/\tau_2-1/\tau_1)$ are plotted as a function of N in Fig. 13. Equation (18) is also plotted in this figure. Fitting the theoretical curve to the data required the variation of two parameters, the destruction coefficient A and ND_M. The solid curve represents the best fit and corresponds to a value of $ND_M=0.88\times10^{18}$ (atoms/cc) (cm^2/sec) and a destruction coefficient of $A=0.11$.

Having now determined the rate of loss of $Hg_2(^3O_u^-)$ molecules by diffusion, the volume destruction processes may be considered. Equation (12) may be rewritten as follows:

$$1/\tau_1-D_M[(j_1/R_1)^2+(\pi/L_1)]=B+C_MN^2. \quad (19)$$

On an N^2 plot the right-hand side of Eq. (19) is a straight line with a zero density intercept corresponding to the rate of spontaneous radiation by the $Hg_2(^3O_u^-)$ molecules. The experimental values corresponding to the left hand side of Eq. (19) are plotted against N^2 in Fig. 14. On the basis of these data it seems plausible that a spontaneous radiation as assumed in the theory does exist, and the lifetime of $Hg_2(^3O_u^-)$ with regard to this radiation appears to be about one-twentieth of a second.

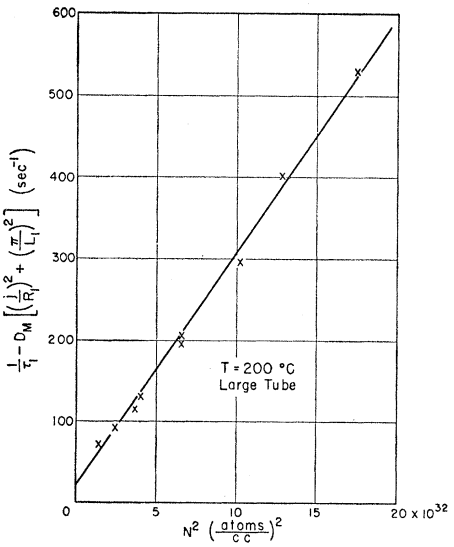

FIG. 14. The volume destruction of diatomic mercury molecules. The zero density intercept corresponds to a spontaneous radiation rate of 20 sec^{-1}.

According to Eq. (12) the rate of collision induced radiation is proportional to N^2 while the spontaneous radiation rate is independent of density. The ratio of the intensities of the two bands may therefore be written as follows:

$$I(4850)/I(3350)\propto C_MN^2/B. \quad (20)$$

The factor of proportionality required to make this relation an equation depends upon the spectral response of the photomultiplier and the optical filters used to resolve the bands, as well as the spectral distribution of the radiation. Since these quantities have not been evaluated, a comparison of a value of C_M/B obtained from Fig. 9 with the value obtained from Fig. 14 has not been made. On the other hand, the intensity ratios have been measured as a function of density. While the straight line in Fig. 9 does not quite intersect the origin, and there is a small unexplained curvature at the lowest densities, it is evident that $I(4850)/I(3350)$ is proportional to N^2 over the major part of the density range.

From the slopes of the curves in Figs. 12 and 14 the three-body collision coefficients, $C_m=100\times10^{-32}$ (atoms/cc)$^{-2}$ sec^{-1} and $C_M=21\times10^{-32}$ (atoms/cc)$^{-2}$ sec^{-1}, have been obtained for reactions (3) and (5), respectively. These coefficients can be compared with those for similar reactions which have been reported in the literature. Phelps and Molnar[23] have found that helium, neon, and argon metastable atoms are destroyed in three-body collisions with the parent gas atoms. The coefficients in these cases vary from 0.02 $\times10^{-32}$ (atoms/cc)$^{-2}$ sec^{-1} for $He(^3S_0)$ to 0.9×10^{-32} (atoms/cc)$^{-2}$ sec^{-1} for $A(^3P_2)$. These values were measured at room temperature while the mercury coefficients given above were obtained at 200°C. In recombination studies three-body collision coefficients of the order of 10^{-32} (atoms/cc)$^{-2}$ sec^{-1} have been observed in hydrogen[24] and also in iodine[25–27] when noble gases are present. When more complex additives are available as third bodies, iodine recombines at a much greater rate, e.g., 138×10^{-32} (molecules/cc)$^{-2}$ sec^{-1} when CH_3CH_2I is present. Finally, Phelps and Brown[28] have measured a three-body coefficient of 6.5×10^{-32} (ions/cc)$^{-2}$ sec^{-1} for the reaction $He^+ + 2He \rightarrow He_2^+ + He$

[23] A. V. Phelps and J. P. Molnar, Phys. Rev. **89**, 1202 (1953). The author is indebted to A. V. Phelps for a discussion of the available experimental results pertaining to three-body reactions.
[24] I. Amdur, J. Am. Chem. Soc. **60**, 2347 (1938).
[25] Christie, Norrish, and Porter, Proc. Roy. Soc. (London) **A216**, 152 (1953).
[26] R. Marshall and N. Davidson, J. Chem. Phys. **21**, 659 (1953).
[27] H. E. Russell and J. Simons, Proc. Roy. Soc. (London) **A217**, 271 (1953).
[28] A. V. Phelps and S. C. Brown, Phys. Rev. **86**, 102 (1952).

at room temperature. A suitable theory for three-body collision processes is not yet available.

It is of interest to consider briefly some of the potential energy curves for Hg_2 in view of the identification of the 3350A band with electronic transitions from the $Hg(^3O_u^-)$ state to the ground state. The curves suggested by the new results are given in Fig. 15. On the right, at large internuclear separation, the states of the separated atoms are specified. At intermediate nuclear separation, the molecular states are identified by the notation appropriate to Hund's coupling case (c).[29] At small internuclear separations the states are specified by Hund's case (a). The correlations between the molecular states and the states of the excited atoms are given by Mulliken.[30]

The ground state of Hg_2 is characteristic of van der Waals molecules in which the relatively weak binding is due to polarization forces. The known properties of this state are summarized by Finkelnburg.[31] The dissociation energy is about 0.08 electron volt and the potential minimum occurs at a nuclear separation of about 3A.

Some quantitative information concerning the $Hg_2(^3\Pi_u)$ state has been obtained by Kuhn and Freudenberg.[32] These authors measured the properties of the absorption band which begins at the 2537A atomic line and extends in the long wave direction to a limit at 3300A. It was found that the intensity of absorption at the long wave limit increases with the square of the atomic vapor density and with temperature, indicating that positive energy levels of the molecular ground state are responsible for the absorption. It was assumed that these positive energy levels are populated according to the Maxwell-Boltzman law and that absorption at the long wave limit involves transitions to the minimum of the $Hg_2(^3\Pi_u)$ potential curve in accordance with the Frank-Condon principle. On this basis the position of the potential minimum of the $Hg_2(^3\Pi_u)$ curve was calculated to be directly above the 0.27 electron volt point on the ground-state curve. From the value of the long wave limit and the wavelength of the atomic line, $Hg(^3P_1) \rightarrow Hg(^1S_0)$, it was determined that the dissociation energy of $Hg_2(^3\Pi_u)$ is 0.84 electron volt.

The $Hg_2(^3O_u^-)$ potential curve has been added to the diagram in a manner consistent with the results of the present paper. It has been assumed that the minimum of the $Hg_2(^3O_u^-)$ curve lies beneath the minimum of the $Hg_2(^3\Pi_u)$ curve. This procedure is based upon the recognition that at small internuclear separation spin-orbit interaction becomes a small perturbation and the two potential curves must approach each other very closely; it seems reasonable that for increasing internuclear distance the spin-orbit energy separation of the two curves increases monotonically to the value for the separated atoms. Using, therefore, the 0.27-electron volt level of the ground potential curve as the final state for the 3350A emission, it follows from the known energy of the $^3P_0$ atomic state that the dissociation energy of $Hg_2(^3O_u^-)$ is 0.71 electron volt.

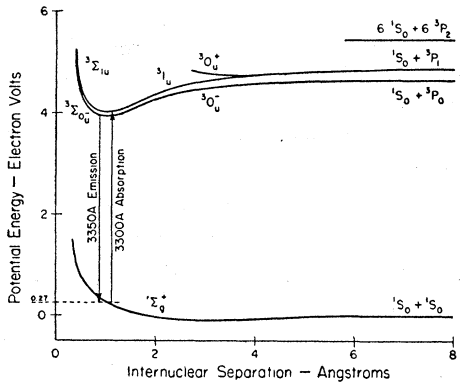

FIG. 15. The potential energy levels of Hg_2 constructed on the basis of considerations discussed in the text.

V. SUMMARY

The intensities of the principal fluorescent bands of mercury excited by the 2537A atomic resonance line have been measured quantitatively as a function of time in the afterglow. Observations have been made at a fixed vapor temperature and over a range of vapor densities within which the character of the fluorescence goes through extensive alteration. The results of the experiments reveal that the two principal bands centered at 3350A and 4850A, have their origin in a common metastable reservoir. The time structure of the afterglow indicates that a second, nonradiating metastable entity is also present. The density dependence of the persistence times and the relative band intensities suggest that three-body collision processes are involved in the chain of events leading to fluorescence.

The experimental results have led to an interpretation in which mercury atoms in the resonance $Hg(^3P_1)$ state are converted to metastable $Hg(^3P_0)$ atoms by quenching collisions with normal mercury atoms. Some of the metastable atoms are then converted to metastable diatomic $Hg_2(^3O_u^-)$ molecules by three-body collisions involving two normal atoms. The 3350A component of the fluorescence is considered to be spontaneous radiation from the molecules; the 4850A compoponent arises from a three-body collision induced radiation process involving two normal mercury atoms.

A detailed analysis based upon this scheme has made it possible to obtain from the data diffusion coefficients for the metastable molecules and the metastable atoms, the lifetime of the metastable molecules with respect to spontaneous radiation, and the frequencies of the three-body collision processes responsible for the

[29] The various angular momentum coupling cases for diatomic molecules are described in G. Herzberg, *Spectra of Diatomic Molecules* (D. Van Nostrand Company, New York, 1950).

[30] R. S. Mulliken, Revs. Modern Phys. 2, 92 (1930).

[31] W. Finkelnburg, *Kontinuierliche Spektren* (Julius Springer, Berlin, 1938).

[32] H. Kuhn and K. Freudenberg, Z. Physik 76, 38 (1932).

annihilation of both the metastable molecules and the metastable atoms. The diffusion coefficient of the metastable atom is in good agreement with the results of other work. The three-body collision frequencies are comparable with those obtained for similar reactions in other gases.

VI. ACKNOWLEDGMENT

It is a pleasure to acknowledge the help of several individuals during the course of this work. Dr. T. Holstein, who first recognized the interesting nature of the problem, guided the theoretical interpretation of the experimental results. Dr. D. Alpert has maintained an interest in the program since its inception and has contributed many helpful discussions. C. G. Matland assisted with the preparation of the experimental tubes and also helped with the tedious task of taking data. Finally, seminar discussions with the members of the Physics Department of the Westinghouse Research Laboratories have been invaluable.

PHYSICAL REVIEW VOLUME 93, NUMBER 6 MARCH 15, 1954

Dipole and Quadrupole Transition Probabilities in Neutron-Capture Gamma Radiation

B. B. KINSEY AND G. A. BARTHOLOMEW
Physics Division, Atomic Energy of Canada Limited, Chalk River, Ontario, Canada
(Received November 30, 1953)

An analysis of the intensities of neutron-capture γ rays in even-charge nuclei shows that at high energies the emission probability of $E1$ radiation is greater than that of any other multipole order. This conclusion is supported by additional evidence from odd-charge nuclei. In three nuclei (Mg^{25}, Si^{29}, and S^{33}) a direct comparison shows that (at the same energy) the emission probability of $E1$ is 200 times greater than that of $M1$ radiation. The rate of emission of $E2$ radiation has been compared directly with $E1$ radiation in only one instance, *viz.*, Mg^{25}, where (at 7 Mev) it was found to be lower by a factor of 2000. Further evidence is adduced to show that this ratio is not exceptional and that the rate of emission of $E2$ radiation (at 7 Mev) is less than that of $M1$ radiation. The absolute rates of emission for $E1$ and $M1$ γ rays are evaluated in those instances where the radiation width of the capturing state is known. When corrected for the level spacing near the initial state (and for the nuclear radius, in the case of $E1$ radiation), the rates of emission are remarkably constant; they are independent of the nuclear charge and mass over a range where the level spacing may vary by a factor of 10^4 or more. The emission rates of $E1$ and $M1$ radiation are generally ten times lower than those predicted by the formula of Weisskopf, which is based on the independent-particle model. The emission rates do not exceed those expected from that formula in the case of the exceptionally strong $M1$ ground-state γ rays from F^{20} and Al^{28}. It is shown that the identification of the spins and parities of excited states in many nuclei can be made on the basis of intensity measurements. Finally, the influence of closed shells on the γ-ray spectra is discussed.

INTRODUCTION

A DETERMINATION of the relative emission probabilities of different multipole orders of γ radiation is of considerable interest for it throws a direct light on the mechanism responsible for the emission of radiation. In the absence of selection rules or other limitations, one would expect that the probability of detection of low-energy electric dipole ($E1$) radiation,[1] would far exceed that of higher multipole orders, for, theoretically, the relative probabilities of emission of the various multipoles should decrease by successive factors of the order of $(R/\lambda)^2$, where R is a quantity of the order of the nuclear radius and $2\pi\lambda$ is the wavelength of the radiation. For 1-Mev radiation and for a nucleus of mass 100, this factor is about 0.1 percent.

Now the greater part of the experimental data on the relative rates of emission of the various multipoles has been derived from the study of the γ rays following β decay. It became increasingly apparent that, among the observed γ rays, far more are of $M1$ and $E2$ types than $E1$. Until recently, this fact has not been fully appreciated because of the tendency of early experimenters working with the heavy elements to obtain internal photoelectric conversion coefficients which were too low. Since the coefficients increase with increasing multipole order, and since they are generally greater for magnetic than for electric radiations, $E2$ radiations were mistaken for $E1$, and $M1$ radiations for $E2$. That these radiations are actually $E2$ and $M1$ is confirmed by more exact calculations[2] of internal conversion coefficients which have given results which are lower than early estimates.[3] Consequently, the few examples of $E1$ radiations following β decay have become fewer still, and, although some well-authenticated

[1] We follow here the notation for electric and magnetic multipole radiation introduced by M. Goldhaber and A. W. Sunyar, Phys. Rev. 83, 906 (1951).

[2] Rose, Goertzel, and Spinrad, Phys. Rev. 83, 79 (1951).

[3] H. R. Hulme, Proc. Roy. Soc. (London) A138, 643 (1932); H. M. Taylor and N. F. Mott, Proc. Roy. Soc. (London) A138, 665 (1932); J. B. Fisk and H. M. Taylor, Proc. Roy. Soc. (London) A143, 274 (1933); A146, 178 (1934); H. M. Taylor, Proc. Cambridge Phil. Soc. 32, 291 (1936).

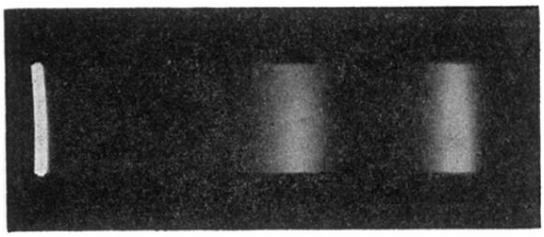

FIG. 1. The band fluorescence of mercury vapor at a density of about 6×10^{16} atoms/cc. The line on the left is the 2537A exciting line; the center band extends from about 3000A to 3700A with maximum intensity at 3350A; the band on the right extends from 4000A to 5300A with maximum intensity at 4850A.

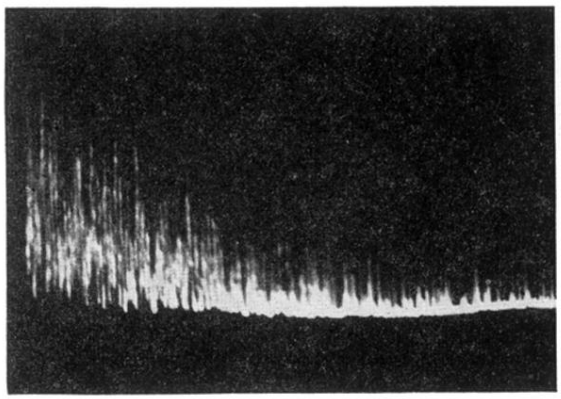

FIG. 5. An oscilloscope trace of a fluorescence decay cycle. The shot effect is due to the random arrival of optical quanta at the photomultiplier. The trace in this photo is about 30 milliseconds long.